CHAPTER

5 Surface versus bulk recombination in state-of-the-art OPV

Abstract

Non-geminate recombination is an important loss mechanism in state-of-the-art organic photovoltaic devices. However, surface recombination and bimolecular recombination are not yet well understood. Therefore, we investigate the interplay between these recombination pathways, by performing drift-diffusion simulations of organic solar cells. First, we make an analytical approximation for the lower limit of surface recombination in organic solar cells. Next, our simulations show that the effect of surface recombination is only notable when bimolecular recombination is weak. For devices with excellent charge transport characteristics, the effect of reducing surface recombination is compensated by an increase in bimolecular recombination. The use of charge carrier blocking layers prevents surface recombination, and reduces bulk recombination near the electrodes when the bimolecular recombination rate is high. We conclude that reducing surface recombination velocities may slightly reduce recombination losses in state-of-the art organic solar cells, but the effect is limited.

N. J. van der Kaap and L. J. A. Koster, *Surface versus bulk recombination instate-of-the-art organic bulk heterojunction solar cells*, Submitted

5.1 Introduction

Previous theoretical work on surface recombination has mainly focused on changes in open circuit voltage V_{OC}, short circuit current I_{SC} and PCE when varying the surface recombination velocities and extraction barriers, while keeping all other parameters constant [53–55]. However, bimolecular recombination and surface recombination cannot be investigated separately. For instance, adjusting bimolecular recombination parameters such as device thickness, mobility or relative recombination strength results in different carrier densities in the device, changing surface recombination as well. This makes it difficult to interpret the present theoretical results for real devices with a wide variety of device parameters. Moreover, experimental determination of the surface recombination dynamics at metallic electrodes is currently not possible, making it unclear to what extent real devices are limited by surface recombination. The only experimental method for adjusting the surface recombination dynamics is the addition of electron- and hole blocking layers that prevent carriers from being extracted at the wrong contact [150, 151]. Although the addition of these blocking layers has resulted in improved PCE's, their operating mechanism is not fully understood yet. Our work is motivated by the current view on the operation of charge carrier blocking layers: preventing minority charge carrier extraction at the electrodes. In order to determine how much state-of-the-art OPV devices can benefit from reducing surface recombination velocities, a more detailed study is required into the interplay between the different recombination pathways and the operation mechanism.

In this chapter, we study the interplay between surface recombination and bimolecular recombination. This process is complicated by the lack of experimental methods for separating the contributions due to bulk and surface recombination. Therefore, we use numerical drift-diffusion simulations to investigate this subject theoretically. Since state-of-the-art devices contain ohmic contacts that do not limit transport, majority surface recombination is very fast, and does not limit device performance. Therefore, we only include the effect of varying minority surface recombination velocities.

First, we use space charge limited theory to derive a lower limit of the minority surface recombination velocity in BHJ solar cells. Next, we perform numerical drift-diffusion simulations to investigate the interplay between bulk recombination and surface recombination in state-of-the-art BHJ solar cells. In order to generalize these results, we compare drift-diffusion simulations of a large number of solar cells that each have different parameters [37]. Then, we discuss the operating mechanism of

Parameter	Value	
ϵ_r	4.0	
N_c	2.5×10^{26}	m^{-3}
T	300	K
E_g	1.2	eV
Generation rate	10^{28}	$m^{-3}\ s^{-1}$
Thickness	100	nm

Table 5.1: Common parameters for the drift-diffusion simulation.

charge blocking layers, and their effect on surface recombination and bimolecular recombination. Even though the addition of charge blocking layers improves the performance of BHJ solar cells, we find that this enhancement is not caused by a reduction in surface recombination. Finally, we conclude that the impact of surface recombination on the performance of state-of-the-art BHJ solar cells is limited.

5.2 Methods

The charge transport characteristics of organic BHJ solar cells are obtained from a numerical drift-diffusion simulation [63]. This simulation solves the coupled Poisson and continuity equations, and calculates the current voltage characteristics under illuminated conditions [37]. The model assumes mobilities that are independent of electric field and charge carrier density. For the boundary conditions, Ohmic contacts are assumed with infinite majority surface recombination velocities, and variable minority surface recombination velocities according to Eq. 1.8. Here, $S = S_n = S_p$ refers to the minority surface recombination velocity that is equal for holes at the cathode and electrons at the anode. Bimolecular recombination is included using Eq. 1.6. A bisection method is used to determine the maximum power point of each device. The constant device parameters are listed in table 5.1.

5.3 Results and discussion

The values of S_n and S_p are hard to determine experimentally, since the interplay between surface recombination and bimolecular recombination cannot be disentangled. Whereas a theoretical upper limit for S_n and S_p was found by Kirchartz *et al.*, a lower limit is not available to date [54]. However, the similarity between single-carrier

diodes and OPV devices can be used to derive a lower limit for the minority surface recombination velocities. Typically, single-carrier diodes feature an Ohmic injecting contact, and a non-Ohmic extracting contact. Thus, the extraction of electrons (holes) at the non-injecting electrode of a single-carrier electron (hole) only diode is analogous to the extraction of electrons (holes) at the anode (cathode) of a BHJ solar cell. Given this similarity, space charge limited theory can be used to develop a simple approximation for the minority surface recombination velocity. Although this approach is only valid in the space charge limited region when the bias $V > V_{OC}$, it should give a rough lower limit for the magnitude of S_n or S_p.

For an electron-only diode, the current density is given by the Mott-Gurney expression [20]:

$$J = \frac{9}{8}\frac{\epsilon\mu_n}{L^3}V^2, \tag{1.5}$$

where μ_n is the electron mobility, ϵ the dielectric constant, and L is the device thickness. The electron density at a distance x from the cathode is given by $\frac{3}{4}\epsilon\frac{V}{qL^{3/2}}x^{-0.5}$ [20]. According to space charge limited theory, the electron density at the anode equals $n_l = \frac{3}{4}\frac{\epsilon V}{qL^2}$. Given that the current at the extracting electrode is given by $J = qS_n(n_l - n_i)$, the surface recombination velocity equals $S_n = \frac{J}{q(n_l - n_i)}$. Substituting the values of J and n_l from space charge limited theory and neglecting n_i, S_n becomes

$$S_n = \frac{3\mu_n V}{2L}. \tag{5.1}$$

For a typical organic solar cell at 1 V above the built-in voltage, this results in a lower limit of S that is close to $1\,\mathrm{m\,s^{-1}}$. This falls well within the limit that was obtained by Kirchartz *et al.* [54], and is close to the region where a decrease in S improves performance [53]. Another feature is that S is not constant, but depends on μ_n: surface recombination velocities will thus increase for high performance devices with large mobilities.

In order to determine the effect of surface recombination on the performance of organic BHJ solar cells, we first investigate the impact of varying the surface recombination velocity on the current-voltage characteristics. Figure 5.1 shows the recombination losses in a typical BHJ solar cell as a function of bias for different surface recombination velocities S. These losses are divided into a bimolecular recombination current density $J_B(V)$ (dotted line), and the surface recombination current densities $J_S(V)$ (solid lines). Because the bimolecular recombination current densities for different S are almost equal, only the values for $S = \infty\,\mathrm{ms^{-1}}$ are shown. For this plot, $\mu_e = \mu_h = 10^{-6}\,\mathrm{m^2\,V^{-1}\,s^{-1}}$, $\gamma = 10^{-3}$, generation rate $G = 10^{28}\,\mathrm{m^{-3}\,s^{-1}}$. The total

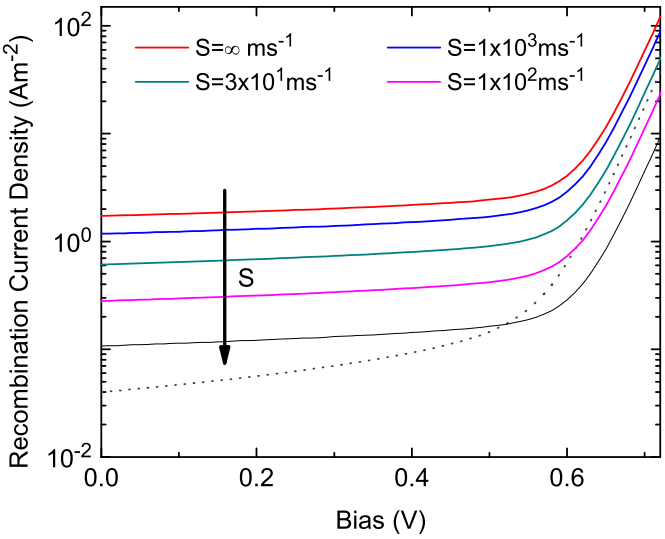

Figure 5.1: Surface recombination current density for different $S_{n,p}$ (solid lines), compared to the bimolecular recombination current density (dotted line). For high $S_{n,p}$, surface recombination will limit both V_{OC} and the short circuit current density J_{SC}. For decreasing $S_{n,p}$, bimolecular recombination becomes the limiting factor for the V_{OC}, while even lower values of $S_{n,p}$ are required to make bimolecular recombination the limiting processes for to J_{SC}.

photocurrent density is given by $J_{Ph} = J_{SC} - J_B(V) - J_S(V)$. For each S, the figure shows $J_S(V)$ and $J_B(V)$: the mechanism with the larger value is the major loss mechanism at V. When S is large, $J_S(V) > J_B(V)$, and both the open-circuit voltage and the short-circuit current are limited by surface recombination. For decreasing S, $J_S(V)$ will first cross $J_B(V)$ at high V, thus increasing the open-circuit voltage and making bimolecular recombination the limiting recombination mechanism. A further decrease of S improves the short-circuit current, until $J_S(V)$ lies completely below $J_B(V)$.

This result explains the correlation between S, the open-circuit voltage, and the short-circuit current that was found by Wagenpfahl *et al.* [53]. However, the impact of surface recombination depends strongly on the bimolecular recombination dynamics: for larger values of γ, J_B will shift upwards, decreasing the effect of surface recombination. Likewise, different mobilities lead to changes in both J_B and J_S. These

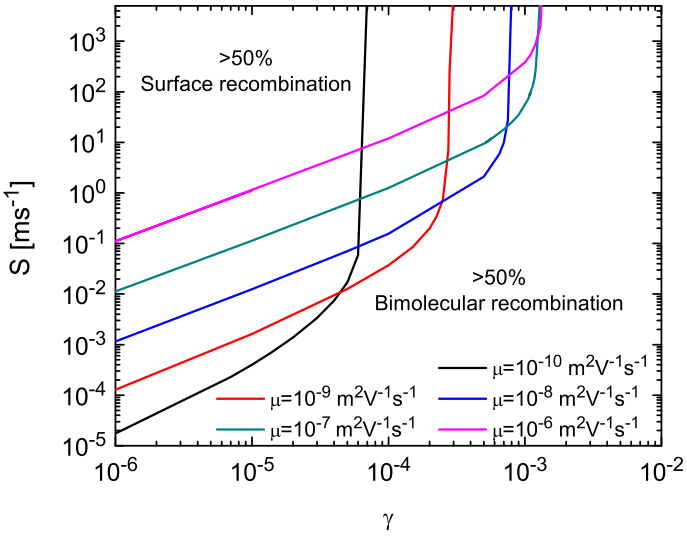

Figure 5.2: Bimolecular recombination strength γ versus the surface recombination velocity S at which both mechanisms are responsible for an equal amount of loss in photogenerated current at the maximum power point. The lines correspond to equal electron and hole mobilities with a value that is indicated in the legend. The region above each line represents the combination of S and γ where surface recombination is dominant, while each combination under the line corresponds to the situation where bimolecular recombination is dominant.

observations agree with the findings of Würfel *et al.* that surface recombination becomes more pronounced when the impact of bimolecular recombination reduces [57].

In order to determine the impact of different γ, S and μ, the following drift-diffusion calculations determine the dominant recombination mechanism for every combination of S and γ. As for the previous calculations, these calculations were performed for equal electron and hole mobilities μ. For each configuration, Fig. 5.2 shows γ as a function of the value of S for which bimolecular and surface recombination losses are equally strong. These calculations were performed at the maximum power point V_{MPP}, since solar cells are typically operated at that bias.

In Fig 5.2, the area above each line indicates all combinations of S and γ for which surface recombination is dominant, while the region under each line represents the

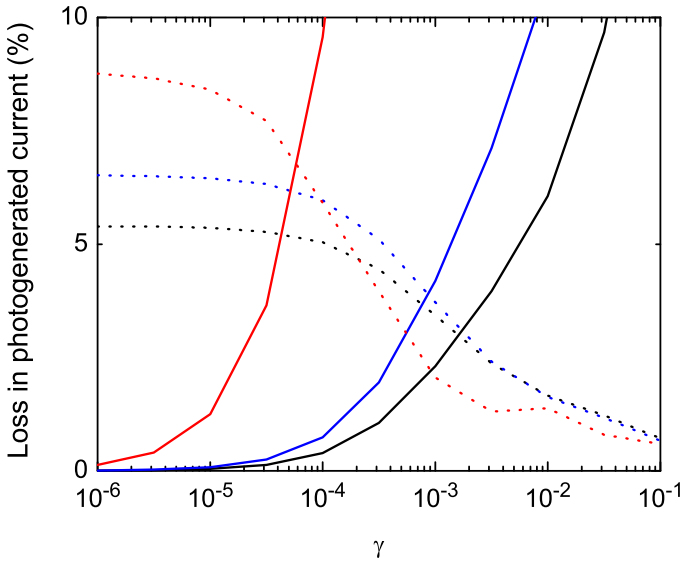

Figure 5.3: The percentage of photogenerated current at the maximum power point that is lost by bimolecular recombination (solid lines) and surface recombination (dotted lines) in case of infinite surface recombination velocities. Equal charge carrier mobilities for electrons and holes are assumed of 10^{-6} m^2 V^{-1} s^{-1} (black lines), 10^{-8} m^2 V^{-1} s^{-1} (blue lines) and 10^{-10} m^2 V^{-1} s^{-1} (red lines).

region where bimolecular recombination is stronger. For varying mobilities and low γ, S scales linearly with μ, since equation 1.6 contains a linear dependence on the sum of the electron and hole mobility. When γ is low, there is a linear dependence between γ and S, this is because J_S and J_B scale linearly with S and γ respectively. This dependence becomes superlinear for increasing γ. As γ is increased further, S will rise to infinity since the contribution due to surface recombination is maximal. The value of γ of this transition decreases for smaller mobilities. This can be explained by the the difference in FF between both cases. When operated at the maximum power point, devices with a high FF feature less recombination losses than devices with a low FF. For increasing mobilities, FF will also increase [143]. Since minority surface recombination does not change at infinite surface recombination velocities, bimolecular recombination in devices with a high mobility is lower than in devices with low mobilities. Therefore, the required value of γ that matches the given amount

of surface recombination is larger than for a device with low mobilities.

Given that state-of-the-art devices possess values of γ that are close to 10^{-3}, and values of $S_{n,p}$ that are close to $1\,\mathrm{m\,s^{-1}}$, surface recombination does not become the dominant recombination pathway. When assuming the upper limit of $10^{3}\,\mathrm{m\,s^{-1}}$ that was found by Kirchartz *et al.* [54], surface recombination will only become dominant for equal electron and hole mobilities higher than $10^{-7}\,\mathrm{m^2\,V^{-1}\,s^{-1}}$. However, most real devices have asymmetric mobilities. Asymmetric charge carrier mobilities result in a slightly lower bimolecular recombination rate at low γ, and a small reduction of V_{OC} compared to the symmetric case. Therefore, the curves in Fig. 5.3 are shifted to the left for these devices. Compared to the symmetric case, the impact of surface recombination is reduced.

When γ reaches values that are smaller than 10^{-3}, surface recombination becomes the dominant loss mechanism for devices with state-of-the-art charge carrier mobilities. Figure 5.3 shows the relative photo current loss of infinitely fast surface recombination and bimolecular recombination for devices with different mobilities, as a function of γ. The maximum loss due to surface recombination decreases with increasing charge carrier mobility, since the charge carrier densities are reduced. Similar to Fig. 5.2, the cross-over point between surface recombination and bimolecular recombination shifts to higher γ for increasing mobilities. Although the relative impact of surface recombination increases for larger mobilities, the absolute loss in performance is reduced.

Whereas the previous calculations focused on the interplay between bimolecular and surface recombination in devices with symmetric mobilities, the following calculation generalizes these results to a broader class of devices. This is done by performing drift-diffusion calculations for a large number of devices with different values for mobility, band gap, γ, S, device thicknesses, and illumination intensities. In order to characterize the recombination dynamics, each calculation stores the losses due to surface recombination and bimolecular recombination at the maximum power point. These results are then compared to the ratio θ between the extraction rate and the recombination rate of the device [143]:

$$\theta = \frac{\gamma G L^4}{\mu_n \mu_p V_{\mathrm{int}}^2} \propto \frac{k_{\mathrm{rec}}}{k_{\mathrm{ex}}}. \tag{5.2}$$

Here, k_{rec} is the recombination rate, k_{ex} is the extraction rate, G is the generation rate, L is the device thickness and V_{int} is the internal voltage of the device. Previously, Barthesaghi *et al.* have shown that a correlation exists between θ and FF [143]. Since

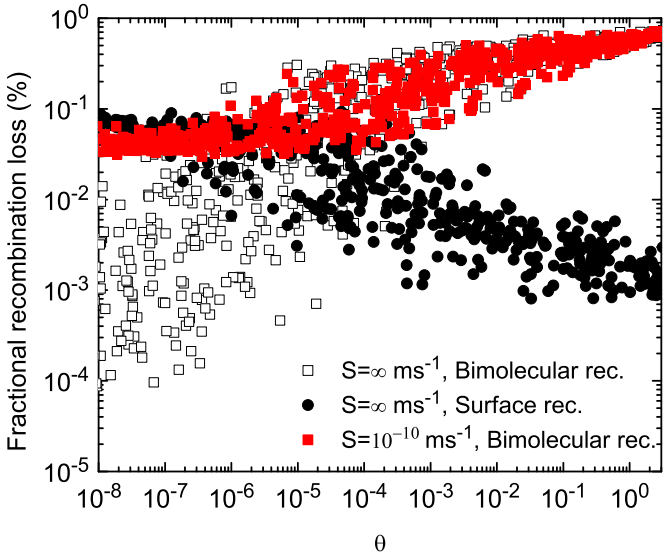

Figure 5.4: Recombination losses at the maximum power point due to surface recombination and bimolecular recombination for a wide range of device parameters. For $S = \infty\,\mathrm{m\,s^{-1}}$, losses due to bimolecular recombination vanish at low θ, while surface recombination losses converge to an upper limit. For very low S, surface recombination losses vanish (not shown), and bimolecular losses increases to obtain the fundamental limit for devices with excellent charge transport characteristics [152].

FF is related to the recombination losses at the maximum power point, it makes θ a good parameter to compare the recombination rates of different devices. The range of all parameters is shown in Table 5.2.

Figure 5.4 shows the fractional recombination losses due to bimolecular and surface recombination at the maximum power point of 1,600 devices for $S = \infty\,\mathrm{m\,s^{-1}}$ and $10^{-10}\,\mathrm{m\,s^{-1}}$. For $S = \infty\,\mathrm{m\,s^{-1}}$ and large θ, bimolecular recombination is the dominating recombination process. When reducing θ by increasing the mobilities or decreasing γ, the contribution due to bimolecular recombination decreases, while surface recombination increases. For $\theta < 10^{-6}$, surface recombination is responsible for all recombination in the device. At $S = 10^{-10}\,\mathrm{m\,s^{-1}}$, the fractional loss due to surface recombination become negligibly low. For large values of θ, bimolecular recombination follows the same pattern for $S = \infty\,\mathrm{m\,s^{-1}}$. However, once θ decreases, the fractional

Parameter	Value	
E_g	1.2	eV
μ_n	$10^{-8} \dots 10^{-4}$	$m^2\,V\,s^{-1}$
μ_p	$10^{-8} \dots 10^{-4}$	$m^2\,V\,s^{-1}$
γ	$10^{-5.5} \dots 1$	
Generation rate	$10^{27} \dots 10^{28}$	$m^{-3}\,s^{-1}$
Thickness	$60 \dots 260$	nm

Table 5.2: The range of parameters for the drift-diffusion simulations of figure 5.4.

losses due to bimolecular recombination do not drop below 3%. Although surface recombination is the major loss mechanism when S is large, reducing S results in a shift of surface recombination to bimolecular recombination. This loss arises because of a fundamental limit when charge transport is excellent [152]. Therefore, efforts for reducing S will only result in limited improvements.

Experimentally, the only method for adjusting surface recombination dynamics is by adding and tuning charge carrier blocking layers between the extracting contact and the active layer. These methods have shown to increase the device performance of organic OPV by preventing electrons from reaching the anode, and holes from reaching the cathode of the device [150, 151]. However, the performance increase of $> 50\%$ that was found is much larger than the calculations of Wagenpfahl *et al.* [53]. This suggests that an additional loss process is reduced as well, and that the impact of surface recombination is limited.

The explanation for this behavior is that charge barrier blocking layers also influence the bulk recombination characteristics. To illustrate this, Fig 5.5 shows the charge carrier densities and the bimolecular recombination rate as a function of position, for a BHJ solar cell. The solar cell has equivalent constant mobilities of $10^{-8}\,m^2V^{-1}s^{-1}$, and $\gamma = 10^{-1}$. Here, the solid lines represent the case including charge carrier blocking layers, whereas the dotted lines show the case without blocking layers. The charge carrier mobilities of the blocking layers is equal to that of the active layer, resulting in equivalent distributions of the majority charge carrier densities. It can be seen that the blocking layers prevent minority carriers from reaching the electrodes, thereby reducing the bimolecular recombination rate in the vicinity of the electrodes.

The extent of this effect depends on the characteristics of both the blocking layers and the active layer. For example, different values of γ result in different majority carrier densities near the electrodes, changing the recombination dynamics in this

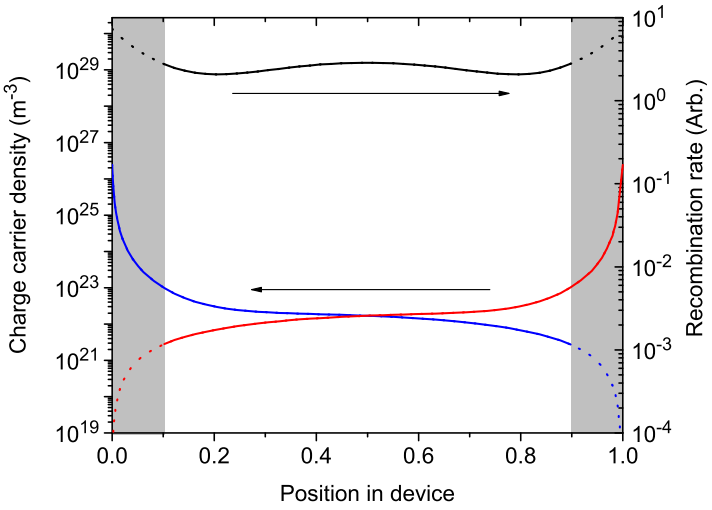

Figure 5.5: Simulated charge carrier distribution of electrons (blue) and holes (red), including (dotted) and excluding (solid) charge blocking layers. The position of the charge blocking layers is indicated by the gray regions. For the case including charge carrier blocking layers, the minority carrier densities disappear near the electrodes. The distribution of the bimolecular recombination rate is shown in by the black lines. For the case including charge blocking layer, the recombination rate vanishes in the gray region.

region. This effect is shown in Fig. 5.6, which visualizes the origin of the bimolecular recombination rate, for solar cells at their maximum power point, for γ values of 10^{-3}, 10^{-2} and 10^{-1}. Although these cells do not contain any blocking layers, introducing these layers prevents recombination in the gray regions. The increased values of γ result in a lower charge carrier densities in the center of the device, whereas the charge carrier densities near the electrodes remain unchanged due to charge carrier injection. Therefore, large values of γ result in increased bimolecular recombination rates near the electrodes. Hence, charge carrier blocking layers are more efficient for solar cells with large values of γ.

The following calculations show the effect of varying the blocking layer thickness on the device performance of BHJ solar cells. Figure 5.7 contains the current-voltage characteristics of a solar cell with similar device parameters, but different blocking layers. The solar cell has symmetric charge carrier mobilities of $1.0 \times 10^{-7}\,\mathrm{m^2\,V^{-1}\,s^{-1}}$,

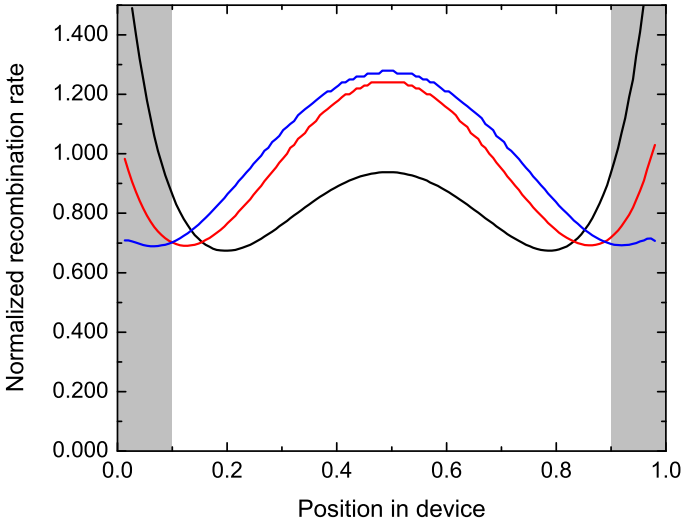

Figure 5.6: Simulated distribution of the bimolecular recombination rate in a 100 nm solar cell with electron and hole mobilities of 10^{-8} m^2 V^{-1} s^{-1}. The distributions are normalized to the overall recombination rate. The lines correspond to different values of the relative recombination strength: 10^{-1} (black line), 10^{-2} (red line) and 10^{-3} (blue line).

Ohmic contacts, an active layer thickness of 60 nm, features a recombination strength of 1, and the generation rate is set to $10^{28}$$m^{-3}$$s^{-1}$. For the blocking layer between the cathode (anode) and the active layer, the same LUMO (HOMO) level is assumed, and a barrier is introduced between the HOMO (LUMO) levels to prevent hole (electron) injection from the active layer into the blocking layer. The charge carrier mobilities of the charge blocking layers are equal to 10^{-7} m^2 V^{-1} s^{-1}. The blue, red and black lines correspond to solar cells with varying blocking layer thickness. The pink line represents a similar solar cell with blocking layers of 1 nm, but has a γ-value of 10^{-3}. The device without blocking layers is a reference device that is subject to both bimolecular and surface recombination. For the device with 1 nm blocking layers, the presence of blocking layers just prevents the extraction of minority carriers at both electrodes. This increases both V_{OC} and J_{SC} slightly, but does not lead to a significant performance enhancement. Finally, the device with 20 nm blocking layers performs

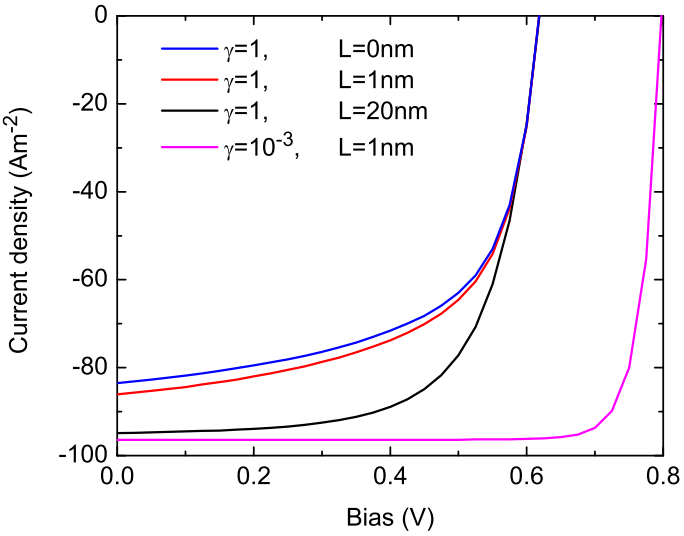

Figure 5.7: The current-voltage characteristics of four solar cells under illumination of $10^{28}\,m^{-3}\,s^{-1}$. The blue line represents a solar cell without charge carrier blocking layers, the red line is a similar device including 1 nm blocking layers on both sides of the active layer, and the black line corresponds to a device including 20 nm thick blocking layers. The pink line corresponds to device with blocking layers of 1 nm, and a value for γ of 10^{-3}.

significantly better than the other two devices: it does not only prevent surface recombination, but it also prevents bimolecular recombination near the electrodes.

The additional increase in efficiency can only be obtained when the recombination dynamics of the active layer are poor. This is confirmed by the device that has 1 nm blocking layers, but features a low value of γ (Fig 5.7, pink line). This device obtains a comparable value of J_{SC} as the device with 20 nm blocking layers and a high value of γ. Therefore, including charge blocking layers will only aid the device performance when bulk recombination dynamics are fast. Moreover, adding charge blocking layers may introduce other issues that limit device performance, such as injection barriers for majority charge carriers, changes in generation profile, and fabrication issues.

5.4 Conclusions

In conclusion, we have performed various calculations to characterize the interplay between bimolecular recombination and surface recombination. First, an approximation for the minority surface recombination velocity in OPV devices was derived using space charge limited theory. Although this derivation was done for single-carrier diodes, the obtained values ($\approx 1\,\mathrm{m\,s^{-1}}$) are well in line with previous estimates of the recombination velocity. According to our approximation, the surface recombination velocity depends on the charge carrier mobility, which means that surface recombination is more pronounced in high performance devices.

Next, we showed the physical mechanism behind the performance enhancement when the minority surface recombination is reduced. Lowering this parameter will first lead to larger values of V_{OC}, while a further decrease results in higher photocurrents. However, the overall impact of reduced surface recombination velocities depends strongly on the bimolecular recombination strength γ. This was shown by determining the recombination parameters for which surface recombination becomes dominant. For a typical charge carrier mobility of $1.0 \times 10^{-8}\,\mathrm{m^2\,V^{-1}\,s^{-1}}$, γ must be equal or smaller than 10^{-3} in order for surface recombination to become important. For decreasing mobilities and reduced surface recombination velocities, γ must be reduced even further.

Bimolecular recombination can only vanish completely when surface recombination is present: there should always be a recombination pathway in order to satisfy the fundamental limit for the current-voltage characteristics when charge transport is excellent. Finally, we have looked into the characteristics of charge blocking layers. Whereas these devices indeed prevent surface recombination, the effects are limited. However, the application of these blocking layers can further improve the device efficiency when recombination dynamics near the electrodes are very fast. This effect reduces when the value of γ decreases below 1.0.

For state-of-the-art organic solar cells, surface recombination is responsible for a limited amount of recombination loss. Reducing the surface recombination velocity will only result in efficiency improvements when the charge carrier mobilities and γ are sufficiently low. Finally, the application of charge blocking layers prevents surface recombination, but a further performance increase is unlikely since γ is typically too low in the active layer.